Imaging Biological Structures with the Cryo Atomic Force Microscope

Yiyi Zhang, Sitong (Jun) Sheng, and Zhifeng Shao
Department of Molecular Physiology and Biological Physics, and Biophysics Graduate Program, University of Virginia School of Medicine, Charlottesville, Virginia 22908 USA

ABSTRACT It has long been recognized that one of the major limitations in biological atomic force microscopy (AFM) is the softness of most biological samples, which are easily deformed or damaged by the AFM tip, because of the high pressure in the contact area, especially from the very sharp tips required for high resolution. Another is the molecular motion present at room temperature due to thermal fluctuation. Using an AFM operated in liquid nitrogen vapor (cryo-AFM), we demonstrate that cryo-AFM can be applied to a large variety of biological samples, from immunoglobulins to DNA to cell surfaces. The resolution achieved with cryo-AFM is much improved when compared with AFM at room temperature with similar specimens, and is comparable to that of cryo-electron microscopy on randomly oriented macromolecules. We will also discuss the technical problems that remain to be solved for achieving even higher resolution with cryo-AFM and other possible applications of this novel technique.

INTRODUCTION

Atomic force microscopy (AFM) (Binnig et al., 1986) has been successfully applied to a variety of biological materials (Engel, 1991; Lindsay, 1993) within just a few years of its invention, primarily for its ability to acquire high-resolution surface images of macromolecules and organelles under nearly native conditions (for recent reviews, see Shao and Yang, 1995; Shao et al., 1995; Hansma and Hoh, 1994; Bustamante et al., 1994). Although nanometer resolution has been demonstrated with several biological samples, such as the cholera toxin and pertussis toxin (Mou et al., 1995b; Yang et al., 1993b, 1994a), as well as bacteriorhodopsin and porin (Muller et al., 1995; Schabert et al., 1995), the resolution of AFM achieved on most other biological specimens has been much lower. For example, on most soluble proteins imaged so far, the AFM only achieved a resolution close to 10 nm (Yang et al., 1994b; Roberts et al., 1995). On the surface of cells, 50 nm was achieved even when the newly invented tapping mode AFM was used (Putman et al., 1994), where the lateral friction due to a scanning tip was mostly eliminated (Hansma et al., 1994). For DNA, the resolution of the double helix pitch was only achieved recently, when DNA was closely packed on a cationic lipid bilayer in solution with a resolution of about 2–3 nm (Mou et al., 1995a). So far the published results strongly support the argument that high-resolution AFM is only obtainable with closely packed, compact molecules (Shao and Yang, 1995). For many other types of biological molecules that cannot achieve close packing or are very flexible, such as antibodies and macromolecular assemblies, reproducible images of even moderate resolution will be very difficult to obtain (Shao et al., 1995; Ill et al., 1993; Roberts et al., 1995; Thimonier et al., 1995).

The difficulty in acquiring useful images of biological structures at room temperature by AFM, and the disappointing resolution achieved on most specimens can, to a large extent, be attributed to the softness of biological samples (Shao and Yang, 1995; Hansma and Hoh, 1994). It has been shown that hydrated proteins could have a Young's modulus as low as 10^5 Pa (Urry, 1988). Therefore, biological structures under the pressure of an AFM tip could be easily deformed or even damaged. Even at sub-nanonewton probe forces, the pressure within the contact area can still be many times the atmospheric pressure. An immediate effect of severe deformation, even without specimen damage, is the loss of surface features in the AFM. Although the image quality is improved with tapping mode AFM because of the elimination of tip-induced lateral movement (Hansma et al., 1994), the absolute probe force applied to the specimen remains on the same order of magnitude at normally used frequencies (Wong and Descouts, 1995). An additional difficulty of imaging in solution is the thermal motion of many flexible macromolecules, as recently indicated by AFM measurements (Thomson et al., 1996). To overcome these difficulties and to improve the fidelity of the methodology, using cryogenic temperatures for AFM imaging has been proposed as a possible alternative (Prater et al., 1991; Yang et al., 1993a; Mou et al., 1993; Shuttack et al., 1994), although the instrumentation would be more complex (Mou et al., 1993) and the elastic properties of macromolecules at low temperatures are not well known (Han et al., 1995). Recently the most notorious problem with cryo-AFM imaging, i.e., surface contamination due to condensation (Prater et al., 1991), was solved with an atomic force microscope immersed in liquid nitrogen vapor (Mou et al., 1993; Han et al., 1995). Based on the measurements with several biological specimens below 100°K, it was shown that the Young's modulus (on the order of 10^{10} Pa, comparable to Indian rubber at room temperature) of both DNA

Received for publication 5 January 1996 and in final form 28 June 1996.
Address reprint requests to Dr. Zhifeng Shao, Department of Physiology, University of Virginia, Box 449, Charlottesville, VA 22908. Tel.: 804-982-0829; Fax: 804-982-1616; E-mail: zs9q@virginia.edu.

0006-3495/96/10/2168/09 $2.00

and proteins was much greater than that at room temperature, providing a necessary foundation for the validity of cryo-AFM in biological imaging (Han et al., 1995). Therefore, deformation and specimen damage can be greatly reduced, resulting in a higher spatial resolution. With the cryo-AFM, not only can the ability to observe dynamic processes be achieved with controlled rapid freezing, other opportunities for biological imaging also become possible. For example, with freeze fracture, the transmembrane domains of an integral membrane protein may be directly elucidated after the extramembrane domains are digested, and the cell surface could be imaged at high resolution with deep etching (Echlin, 1992).

In this paper we present applications of the cryo-AFM to a variety of biological specimens to demonstrate the power and versatility of the cryo-AFM. In addition to applications, we will further discuss the resolution achieved in the cryo-AFM with commercially available cantilevers, and the problems that have not been fully resolved.

MATERIALS AND METHODS

Materials

All chemicals used were reagent grade and were obtained from Sigma Chemicals (St. Louis, MO). Purified immunoglobulins (G, A, M) and α_2-macroglobulin were obtained from Sigma Chemicals, and the purity, according to the supplier, was better than 95%. Red blood cells were prepared from freshly drawn rabbit blood and washed by established procedures (Dodge et al., 1962). Single-stranded plasmid DNA, M13 mp18 (7.2 kb), was prepared according to the procedure described by Sambrook et al. (1989). The yield of ssDNA was determined on DNA agarose gel, and the purity of DNA was examined by the ratio of OD260/OD280.

Instrumentation

The details of the cryo-AFM used in these studies have been published elsewhere (Mou et al., 1993; Han et al., 1995). Briefly, the AFM is operated in liquid nitrogen vapor with an imaging temperature normally in the range of 80–85°K, which can be varied between 77°K and 220°K by controlling the liquid nitrogen level. A pressure slightly higher than the atmospheric pressure must be maintained in the cryogenic dewar. The complete cryo-AFM system built in this laboratory is shown in Fig. 1.

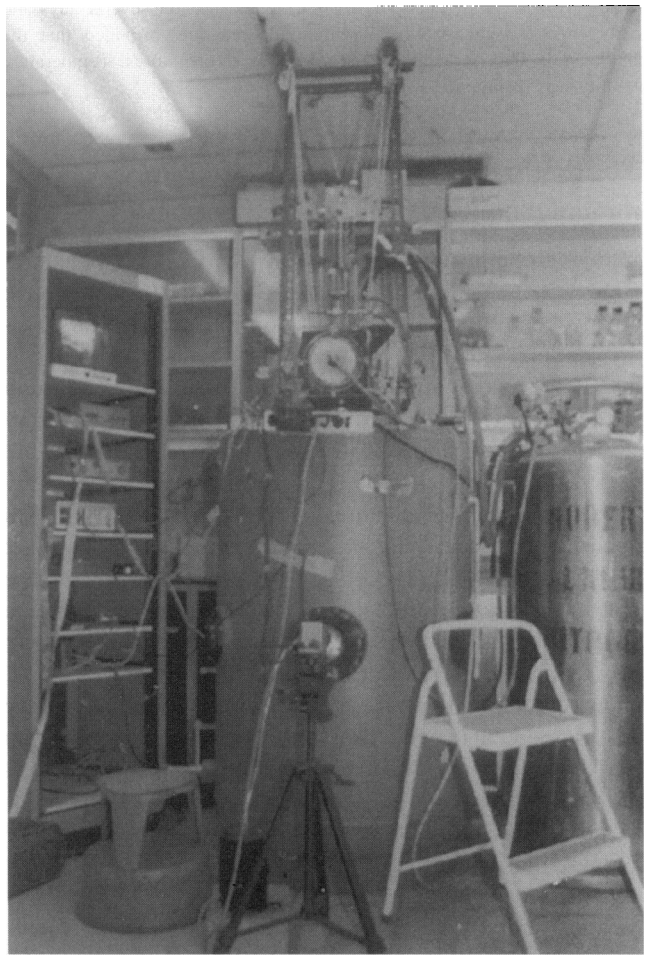

FIGURE 1 The cryo-AFM system developed in this laboratory. The AFM head is operated in liquid nitrogen vapor under a pressure slightly above that of the atmospheric pressure. The specimen preparation/exchange box is seen at the top of the dewar. The AFM is always kept at low temperatures. Both the specimen and the cantilever can be changed in situ. Inside the superinsulated dewar, 100–200 l of liquid nitrogen is maintained. For most operations, an imaging temperature of 80–90°K is maintained. Details of the instrumentation are published elsewhere (Mou et al., 1993; Han et al., 1995). The dewar is about 5 feet tall and weighs more than 600 lb. After the initial operating period (~2 weeks), no contamination was found inside the dewar.

Specimen preparation

A small droplet of solution (~20 μl), containing the appropriate macromolecules (with a concentration in the range of 1–5 μg/ml), was applied to a freshly cleaved mica surface (5 × 5 mm^2) in a clean nitrogen environment. After incubation for a few minutes, the specimen was washed many times with appropriate buffers. It was found that the buffer was an important factor to control to retain these molecules in a native-like conformation, although using deionized water for the last wash did not seem to alter the structure of most molecules within the resolution achieved in these studies (see next section). After the excess solution was removed with a stream of nitrogen (pressurized), the sample was quickly transported into the AFM chamber, which was already at the cryogenic temperature (≤15 s). Any exposure to air, even if very brief, resulted in contaminated samples without high resolution. Prolonged storage in the preparation box, even though it was purged by nitrogen gas continuously, also resulted in specimen deterioration, perhaps because of the residual contaminants. Red blood cells, after washing with phosphate-buffered saline (PBS), were incubated on mica for 2 min. After excess cells were removed with PBS, the sample was lightly fixed with 0.05% glutaraldehyde in PBS for 10 s. Before the sample was frozen, it was further washed with deionized water. The chemical fixation was found necessary to prevent the red blood cells from lysis in the last step. The final removal of the salt from the solution was necessary to avoid excessive surface deposition.

Imaging conditions

All AFM images were obtained with cantilevers purchased from Park Scientific (Sunnyville, CA). These were uncoated cantilevers with oxide sharpened tips. The nominal spring constant was 0.03 N/m at room temperature. Measurements of the shift of the resonant frequencies indicated that the actual spring constant was only about 15% greater at about 100°K when compared with that at room temperature. Typical scanning speed was 1–2 Hz, but 0.2–0.5 Hz was sometimes used to improve the image quality. The adhesion force was normally stable on clean specimens with a typical

value between 1 and 2 nN, and a good tip can last for several days and many engage/disengage cycles without degradation, provided that the cantilever is always maintained at cryogenic temperatures. Temperature stability was maintained within 0.25°K/h.

RESULTS

Immunoglobulins

Immunoglobulins are large, flexible multidomain molecules (Carayannopoulos and Capra, 1993); their structures have already been elucidated by various biochemical and biophysical methods. Despite their broad use in immunolabeling (Polak and Varndell, 1984) and availability at high purity, imaging by AFM in solution or in air was not very successful (Yang et al., 1994b; Ill et al., 1993; Roberts et al., 1995; Thimonier et al., 1995). The best images to date only revealed particulate structures on the substrate surface with much larger dimensions than the known values (Roberts et al., 1995; Ill et al., 1993), and the morphology of these molecules was never resolved by AFM to a resolution comparable to that of electron microscopy (Parkhouse et al., 1970). When these molecules were imaged by cryo-AFM, much higher quality images were readily obtained with only sparsely populated specimens. In Fig. 2 an image of human IgG1, obtained at 85°K, is shown. The well-resolved characteristic Y shape provides not only a useful validation of the cryo-AFM, but also a necessary reference when more complex immunoglobulins are imaged. It is also noted that the structure of IgG1 is rather heterogeneous, indicating that the long hinge region is very flexible. Direct measurements indicate that for the well-resolved Y-shaped IgG1, the overall lateral dimension is 15–16 nm, in good agreement with the known values from electron microscopy and x-ray diffraction (Poljak, 1975). However, the height of the IgG1 is only 2.5 nm, lower than what would be expected (4 nm) in the Y conformation (Poljak, 1975). Although a possible reason for this lower height is the collapse of the molecule during the removal of the solution due to the surface tension of water, a surface adsorbent layer of up to ~1 nm is a more likely explanation for the lower height, based on our previous studies (Han et al., 1995).

When IgA was imaged with the cryo-AFM, with the monoclonal antibody used, in addition to monomers and dimers, higher oligomers were also seen in the AFM images, which was initially a surprise because of the notion that IgA should be primarily dimers. A typical image of monoclonal IgA is shown in Fig. 3 (upper panel) as a stereogram (Shao and Somlyo, 1995). Representative individual molecules of IgA, corresponding to each oligomeric class (up to tetramer), are collected in the lower panels. The overall length of the IgA dimer is about 30 nm, consistent with two IgG subunits in a tail-to-tail configuration. For the IgA tetramer, the diagonal length (measured from two opposing IgG subunits) is ~32 nm, which is also consistent with two IgG subunits. For the IgA trimer, each "arm" measures 15–16 nm, again in general agreement with the dimensions of IgG. It is seen that for many of these molecules, the central J chain appeared to be discernible, which

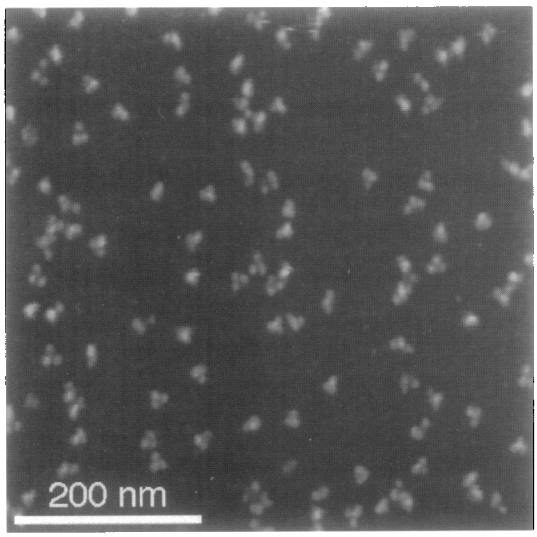

FIGURE 2 A cryo-AFM image of IgG (human IgG1), obtained at about 85°K. The characteristic Y shape of IgG is well resolved. It is also seen that considerable conformational heterogeneity exists, reflecting the flexible nature of this molecule. Similar specimens could not be imaged by the AFM at room temperature, because of the tip-induced movement and molecular flexibility. The sample was very stable at cryogenic temperatures. The lateral dimensions are very close to the known values.

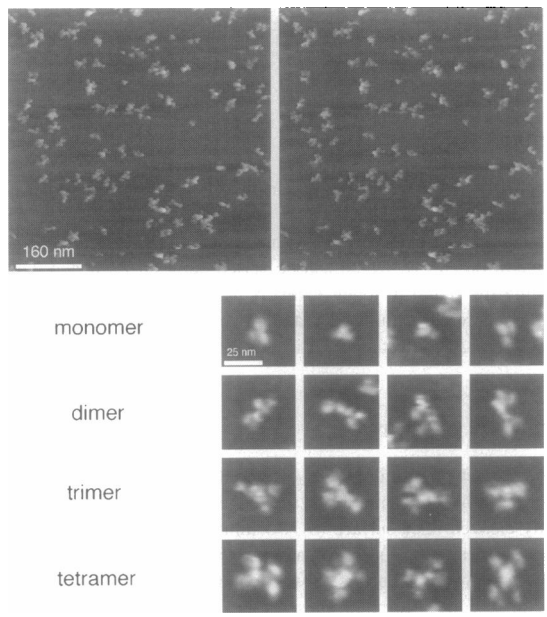

FIGURE 3 A cryo-AFM image of monoclonal IgA (mouse), obtained at 88°K. A stereogram is presented to show the complicated structure. From these images it is immediately recognized that the monoclonal IgA is a mixture of monomers, dimers, trimers, and tetramers, although the existence of higher oligomers cannot be entirely ruled out. It is seen that the dimers are rather flexible, with the small J chain sometimes resolvable (see the lower panel). But the tetramers appeared to be rather rigid, with a symmetrical cross shape. On some of the tetramers, the Fab domains can be seen.

has a nominal molecular weight of 15–20 kDa (Carayannopoulos and Capra, 1993). Although the dimers appeared rather flexible, it is interesting to note that tetramers were more regular, with a flat cross appearance. The Fab domains are also clearly discernible in many IgA molecules. For some unknown reason, there were fewer trimers in these preparations, although the stoichiometry of these oligomers in purified monoclonal antibodies has not been established. These observations are consistent with a recent biochemical study that isolated components up to the size of a tetramer from monoclonal IgA were purified, and the existence of higher oligomers was not eliminated (Vaerman et al., 1995). The smallest feature resolved with these specimens is about 3 nm. It should be mentioned that this is also the first structural elucidation of IgA trimers and tetramers with any direct structural approach. It may be noted that the high contrast obtained in the cryo-AFM also eliminated the need for image averaging, which is not quite applicable to flexible structures.

In a previous publication (Han et al., 1995) we suggested that IgM might have two different conformations. This observation is now confirmed with additional studies, with an example shown in Fig. 4. In addition to the textbook flat pentamer model (with five IgE-like subunits, linked together by disulfide bonds and a J chain), based on negatively stained electron microscopy and other methods (Parkhouse et al., 1970; Perkins et al., 1991), the cryo-AFM images also contained a conformation with a much higher center column and a diameter of 35–45 nm (see Fig. 4, middle panel). Only a small minority showed the flat pentameric form of 45–50 nm diameter, with the small domain in the center appearing to be the J-chain (see Fig. 4, lower panel). Superficially, this form appeared to be more consistent with the results of electron microscopy (Parkhouse et al., 1970; Perkins et al., 1991). However, for the majority of the population, a more compact structure is revealed. It is not clear how to interpret these two different structures (conformations). Further study with limited cross-linking or other manipulations may be useful for constructing a model for the IgM. To appreciate the advantage of cryo-AFM in imaging these large flexible molecules, one should compare the images presented here with those obtained with room temperature AFM (Roberts et al., 1995; Thimonier et al., 1995) and with electron microscopy (Parkhouse et al., 1970). We have attempted imaging of similarly prepared IgM specimens either in air or in propanol at room temperature with the AFM, for the purpose of a direct comparison with those obtained at cryogenic temperatures. Unfortunately, no stable and reproducible images could be obtained under these conditions. The major problem was that the IgM molecules were simply swept aside during scanning and broke into smaller pieces. A similar experience was also reported in the early period of biological AFM research.

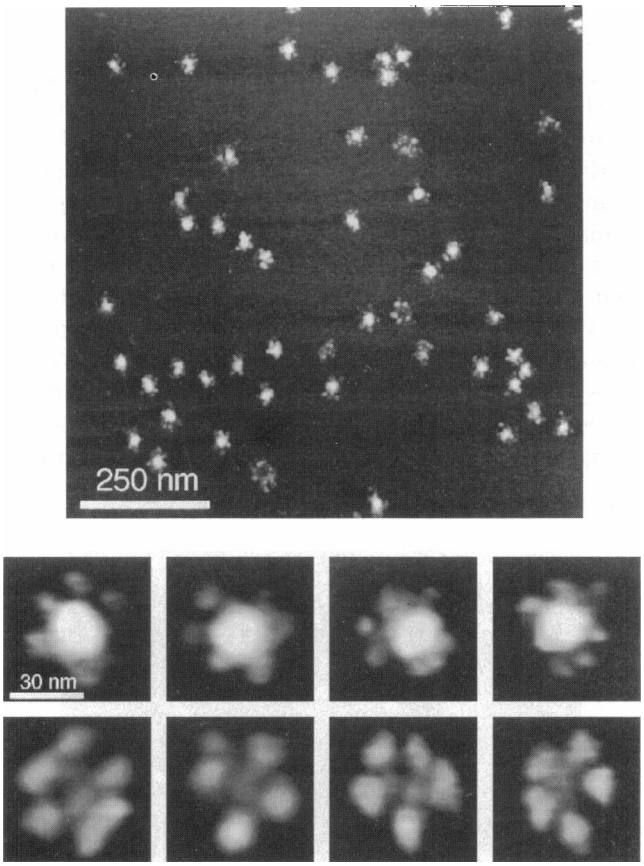

FIGURE 4 A cryo-AFM image of monoclonal IgM (mouse), obtained at 84°K. The oligomeric structure is well resolved, but the structural heterogeneity is also clearly conveyed. One may notice that the majority of the molecules can be divided into two structures (see the lower panel): one that is planar, where the J chain appears to be discernible (lower panel), and one that has a similar overall dimension but with a higher center (middle panel). For the latter case, part of the Fc domains and the J chain appear to be above the plane of the Fab domains, a conclusion inconsistent with the current IgM model. Further studies may provide useful data for the construction of a spatial model for IgM. It is instructive to compare these images with those obtained with AFM in solution (Roberts et al., 1995; Thimonier et al., 1995) and electron microscopy (Parkhouse et al., 1970).

Human native α_2-macroglobulin

α_2-Macroglobulin (α_2-M) is a plasmatic tetrameric glycoprotein of 720-kDa molecular weight, which is shown to be a potent proteinase inhibitor (Barrett and Starkey, 1973). Despite many electron microscopy studies (Delain et al., 1992), the structure of the native α_2-M remains controversial, with many models proposed to explain the projected images. Recently, cryo-electron microscopy was used to reexamine this large structure (Larquet et al., 1994), and the authors have attempted to unify all proposed models by showing different views of a 3-D model based on reconstruction. It is very likely that structural heterogeneity and molecular flexibility are responsible for the many different models, and the fact that electron micrographs are only a 2-D projection of the 3-D structure further complicated the interpretation of the results.

A 3-D surface image may be helpful in establishing necessary constraints for 3-D reconstruction.

Native human α_2-M was readily imaged in the cryo-AFM, with a resolution comparable to that of cryo-electron microscopy, i.e., 4–5 nm (Larquet et al., 1994). In Fig. 5, nearly all views corresponding to that of the 3-D model (Larquet et al., 1994) can be identified without image averaging. Structural heterogeneity is clearly conveyed in these images, indicating the difficulty in obtaining much higher resolution with image processing. A number of "typical views" are collected in the lower panels of Fig. 5. The tetramer can be clearly seen in some of these views. Although without a detailed image reconstruction it is difficult to compare these results with those of electron microscopy (Larquet et al., 1994) with absolute certainty, the overall lateral dimensions (30–40 nm) are consistently larger than those from most electron microscopy studies, although it is in reasonable agreement with the dimension of a related protein, ovomacroglobulin, which has a subunit composition and molecular weight similar to those of α_2-M (Ikai et al., 1990). To eliminate the possibility that the molecules were denatured in the preparation, we used 0.01% glutaraldehyde to fix the α_2-M after adsorption. We found no significant morphological differences between fixed and unfixed specimens. The dimensions remained essentially the same. Therefore, the larger size determined by the cryo-AFM was not due to possible denaturation of the proteins in the preparation process. It is also unlikely that the substrate interaction was responsible for the increased size (causing flattening of α_2-M on mica), because even with negatively stained electron microscopy, α_2-M was also on a supporting carbon film. One possible explanation for the discrepancy is that only the core of each subunit was visible by electron microscopy (either with staining or frozen hydrated), whereas the surface of α_2-M was imaged in AFM, even if the surface mass density was much lower. The tip convolution could also contribute to the larger size, but its effect has been much smaller with other specimens of a comparable molecular weight. It will be interesting to compare the native structure with that of the substrate bound form, where the structure appeared to be more homogeneous based on electron microscopy (Marshall et al., 1992) and low-resolution x-ray diffraction (Anderson et al., 1995).

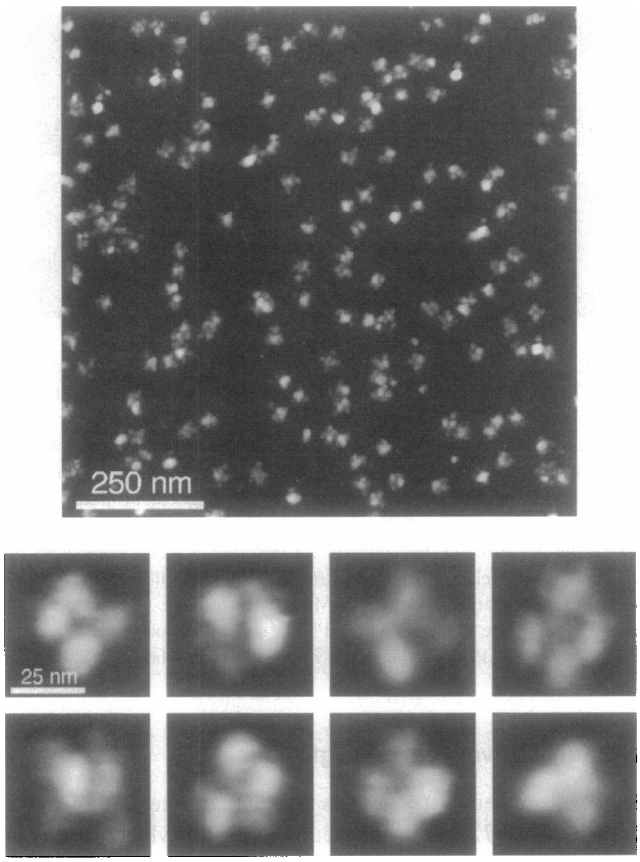

FIGURE 5 A cryo-AFM image of the native human α_2-macroglobulin, obtained at 84°K. Almost all orientations are found in this image. Several typical orientations are collected in the lower panels, which correspond well to the structure based on cryoelectron microscopy and 3-D reconstruction (Larquet et al., 1994). The tetramer is well resolved in some of these images. It may be also noted that the AFM image has a slightly higher resolution toward the periphery of the molecule, which was not well resolved in the electron micrograph because of the random orientation of α_2-M. Because the AFM is already a surface image, the information obtained here provides additional boundary conditions for the 3-D reconstruction. Studies on other large molecular assemblies should be equally beneficial. The lateral dimensions obtained by cryo-AFM are consistently larger (~30 nm) than those obtained with electron microscopy. Cross-linking did not change this conclusion (see text for discussion).

Nucleic acids

Plasmid DNA has been a favorite with AFM imaging, because of its stable structure upon dehydration and its easily recognizable circular form (Bustamante et al., 1993). Such specimens were also very stable in cryo-AFM. In a previous publication (Han et al., 1995) we have shown that the best resolution achieved by cryo-AFM was slightly less than 3 nm, which is some improvement when compared with that in air, where 6–10 nm was often achieved (Yang et al., 1992; Bustamante et al., 1992). However, the pitch of the double helix was not consistently resolved by cryo-AFM (Han et al., 1995), which has been seen by AFM in solution with closely packed dsDNA on cationic lipid bilayers (Mou et al., 1995a). We suggest that this limited resolution of cryo-AFM on DNA is primarily due to specimen preparation, where adsorbed water and other molecules were solidified at cryogenic temperatures.

We have further applied cryo-AFM to image single-stranded DNA. An example is shown in Fig. 6, where the single-stranded plasmid M13 was imaged. In the presence of Mg^{2+}, M13 appeared in a compact form with a lateral dimension in the range of 150–300 nm. The resolution shown is about 4–5 nm, higher than that obtained with the tapping mode AFM in solution (Hansma et al., 1995). As in the case of IgM, we were unable to obtain useful images with ssDNA in air at room temperature. These results indi-

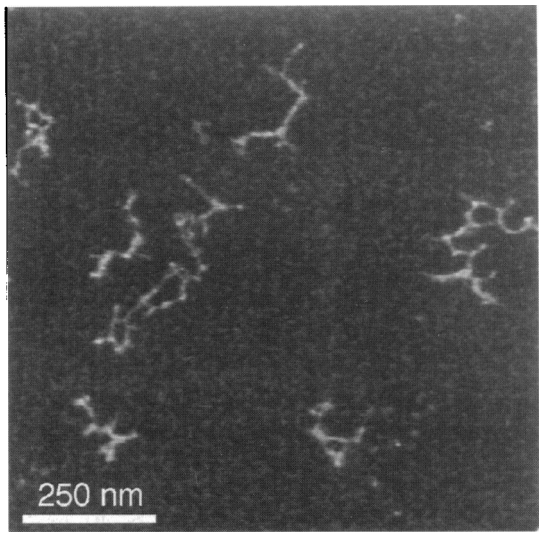

FIGURE 6 A cryo-AFM image of single-stranded plasmid M13 obtained at 84°K. The resolution achieved on these samples is about 4–5 nm, higher than that by the tapping mode AFM in solution. The compact conformation is expected, because of the presence of Mg^{2+} and complementary sequences. The overall dimensions are in the range of 150–300 nm, consistent with other studies. Based on these results, the stem-loop conformation of many RNA molecules should be resolvable.

cate that cryo-AFM is particularly suitable for the study of RNA, which is easily degraded in solution, and perhaps even the ribozymes, where the structure could be "fixed" at cryogenic temperatures. In fact, information regarding the ribozyme's higher order structure under different conditions is still very limited at present (Wang and Cech, 1992).

Red blood cell surface

The ability to image the cell surface at high resolution can find many applications in cell biology, such as the domain structures of the membrane (Rogers and Glaser, 1993), receptor clustering and protein redistribution in response to various stimuli (Metzger, 1992), and endocytosis and exocytosis (Smythe and Warren, 1991). Although the AFM has been successful in imaging live cells in solution (Henderson et al., 1992; Hoh and Schoenenberger, 1994), the resolution achieved on the cell membrane was much lower than that with purified macromolecules and was insufficient to recognize membrane-associated proteins. Cryo-AFM has been shown to be capable of imaging such large structures at high resolution, approaching 2–4 nm in some cases (Han et al., 1995). These results have been confirmed with further experiments. In Fig. 7 the red blood cell was imaged by both scanning electron microscopy (Fig. 7 *A*) and cryo-AFM (Fig. 7, *B* and *C*). To prevent the cells from lysis in the final wash with water, they were fixed with glutaraldehyde for AFM imaging. Although both methods are well suited to resolving the shape of the red blood cells, the resolution of cryo-AFM on the cell surface is much higher (Fig. 7 *C*). The most notable feature on the red blood cell surface is the closed boundaries, which have a lateral dimension generally in the range of several hundred nanometers, which appeared very similar to an earlier observation of red blood cell ghosts (Han et al., 1995). Although the nature of these peculiar surface features has not been identified at present, the membrane domains inferred from particle tracking studies indicated a similar domain size (Sheets et al., 1995). At present, the nature of membrane domains has not been firmly established (Edidin, 1993).

DISCUSSION

Based on the results presented in this study, we have demonstrated that cryo-AFM is a robust and powerful structural tool for the study of a broad range of biological samples

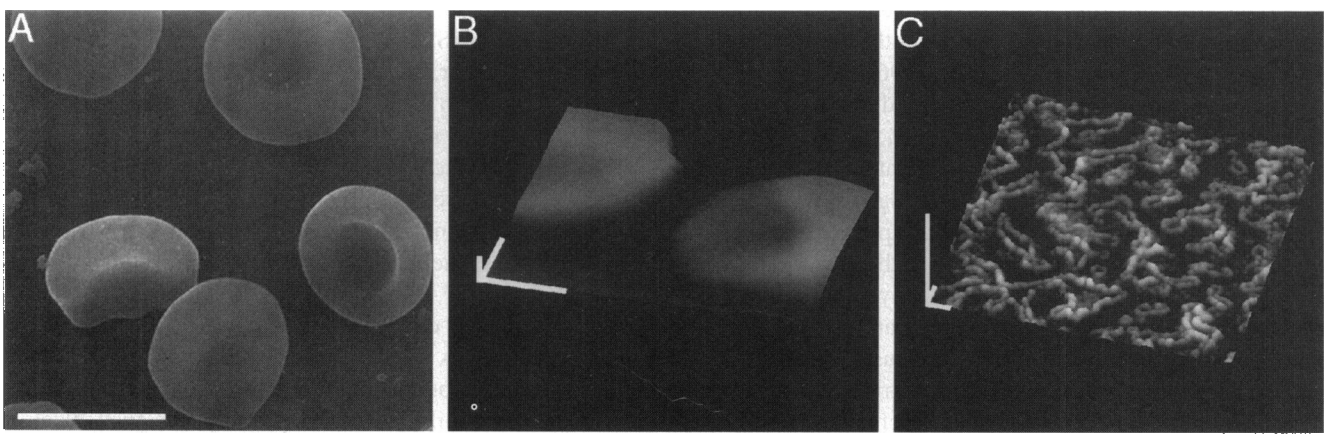

FIGURE 7 Images of red blood cells (from rabbit). (*A*) An SEM image of the red blood cell. Beam voltage was 25 kV and secondary electrons were used for imaging. The cells were lightly fixed before dehydration. The sample was coated by a thin layer of gold to avoid charging. Although the shape of the red blood cell was well resolved, no high-resolution structure on the surface was resolved. Scale bar: 5 μm. (*B*) A cryo-AFM image of the red blood cell. The shape of the red blood cell was also well resolved. Because the maximum z-range of the scanner in our system is only 1.3 μm, part of the image was saturated (flat top), because the maximum thickness for a rabbit red blood cell exceeds 2.5 μm. Scale bar: 1.75 μm (in all three dimensions). (*C*) A high-resolution cryo-AFM image of the red cell surface. It is seen that many more details can now be resolved. Scale bar: 100 nm (in all three dimensions).

with a minimal preparation procedure. For most specimens imaged, cryo-AFM also showed a significant improvement in spatial resolution, when compared with those obtained by the AFM in solution or in air at room temperature. This improvement in resolution can be largely attributed to the much higher specimen stability, the elimination of contamination either on the sample surface or on the AFM tip, and the reduction of molecular motion. However, it is not clear at present whether the greater rigidity is entirely due to the effect of freezing at low temperatures, or whether the possible dehydration also played some role. The failure to obtain stable and reproducible images of similarly prepared specimens in air seems to suggest that the low temperature has played a major role in improving the image quality. Although the answer to this question must await the completion of a freeze etching system for cryo-AFM, it may be useful to point out that complete dehydration is unlikely to be achievable with our procedure, because it was already known that to eliminate water from a mica surface, heating in vacuum is often required (Elmer, 1980). Therefore, it is most likely that a thin layer of frozen solution was always present on the specimen surface, as suggested by the observation that with a much stronger cantilever, a surface layer of up to ~1 nm could be scraped away (Han et al., 1995). This observation could also explain the lower height measured by the cryo-AFM. Another possible problem with even partial dehydration is the denaturation of the proteins, which could lead to structural changes. However, such an effect has not been observed with cryo-AFM, which is consistent with electron microscopy of myosin, where the specimen was dehydrated in vacuum (Flicker et al., 1983), although structural changes cannot be ruled out at higher resolutions. With freeze etch, such problems should be much reduced, if not eliminated.

With the specimens imaged in this paper, the best resolution appears to be ~3 nm (see Fig. 3). (Here the word "resolution" is not well defined, because the resolution in the atomic force microscope is strongly dependent on both the tip geometry and the topology of the specimen (for further discussion, see Shao et al., 1996). Therefore, the word "resolution" should be understood as, perhaps, the "smallest resolvable feature.") However, we must emphasize that the resolution achieved to date is not yet the ultimate resolution of cryo-AFM, judging from the resolution achieved by AFM on some closely packed samples in solution (Mou et al., 1995b). Because of the much improved molecular rigidity, there is no reason why the resolution of cryo-AFM should not reach the sub-nanometer level, at least for well-prepared specimens. Obviously, the method of specimen preparation will be critical to further improvement of the resolution of cryo-AFM. To achieve the highest resolution, the true surface of the specimen must be exposed without any adsorbent layer. From this point of view, a freeze-fractured surface may be most appropriate, where the transmembrane domains of integral membrane proteins can be exposed for imaging, an exciting aspect indeed. In this case, a surface bound layer is unlikely to be a serious problem. But the suitability of deep etching must be carefully examined because of possible surface deposition of salts and other molecules. Based on shadowed electron microscopy, where 4–5 nm resolution has been demonstrated, at least 1–2-nm resolution should be achievable with well-prepared specimens in the cryo atomic force microscope, because the metal shadow should be at least a few nanometers thick (Echlin, 1992). At 1 nm resolution, many structural motifs on the surface might be recognizable. At present, the details of freeze fracture and freeze etching under ambient pressure in nitrogen gas have not been worked out. The expertise accumulated with electron microscopy may not be directly applicable because of the surface contamination in a low-vacuum chamber. The atomic force microscope tip itself can also be further improved, considering that the tip radius of curvature of commercial cantilevers is in the range of 5–40 nm (oxide sharpened tips; Digital Instruments, Santa Barbara, CA). In solution, any initial contamination on the tip could be scraped away during imaging or pushed through with a slightly larger force, because these contaminants are normally soft and weakly attached. In fact, for AFM in solution, one rarely achieves the best resolution with the first frame after tip engagement. It often requires many frames to "condition" the tip before the best resolution can be obtained. Therefore, the high resolution achieved in solution is most likely the result of surface imperfections (Shao and Yang, 1995). But, at cryogenic temperatures, all contaminants may become solidified and firmly attached, resulting in an enlarged tip radius. Small bumps on the tip surface could be completely covered. We have found that prescanning on some polymeric specimens could often improve the resolution of the cryo atomic force microscope if it is performed at the imaging temperature in situ, perhaps because some of the contaminants were removed. Although the tip-related broadening is not apparent in most images presented in this paper (suggesting that small asperities may exist at the tip surface that are responsible for the image contrast; also see Shao et al., 1996), the tip size will always be a limiting factor, provided that specimen damage remains tolerable. Electron beam-deposited super tips (Keller and Chi-Chung, 1992) may be the perfect choice for cryo-AFM, because of the absence of excessive deformation or damage due to the increased pressure (Shao and Yang, 1995), and because tip contamination can be eliminated with a controlled process, such as transfer and storage in clean nitrogen gas. However, the ability to fabricate nanometer-scale tips has not been developed to date. Because a short and sharp single tip is all that is required for cryo-AFM, the available technology should already be adequate, if the procedure is modified with a specially designed electron beam. It is important to appreciate that all of these problems are technical, and the resolution of these problems breaks no fundamental laws of physics or biology.

To conclude, we would like to suggest a particularly interesting future development. It is possible to combine a cryo atomic force microscope with a sectioning device or

another cryo atomic force microscope with a much stronger cantilever. Therefore, after the exposed structure (after etching) is imaged, it could be removed by the atomic force microscope with the stronger cantilever or by a diamond knife before another round of etching. (According to a leading manufacturer of diamond knives, as little as 5 nm could be shaved away with a flatness of ~2 nm.) Repeated application of this procedure will provide a 3-D image of the structure at nanometer resolution. With this ability, the internal structure of large complexes, such as the chromosome or the nucleus, may be revealed, providing spatial information that could not be obtained at present without destroying these structures. The realization of this and other capabilities will inevitably make cryo-AFM a unique, yet powerful, structural approach in biology.

We thank Dr. Jianxun Mou for his contributions in the instrumentation and D. Czajkowsky for a critical reading of the manuscript. We also thank Dr. R. Nakamoto for many helpful discussions and the synthesis of M13, and Dr. A. P. Somlyo for his continued interest in the cryo-AFM project.

The work is supported by grants from the National Institutes of Health (RO1-RR07720 and PO1-HL48807) and the National Science Foundation (BIR-9115655).

REFERENCES

Alberts, B., D. Bray, J. Lewis, M. Raff, K. Roberts and J. Watson. 1994. Molecular Biology of the Cell, 3rd ed. Garland, New York.

Anderson, G. R., T. J. Koch, K. Dolmer, L. Sottrup-Jensen, and J. Nyborg. 1995. Low resolution X-ray structure of methylamine treated α_2-macroglobulin. *J. Biol. Chem.* 270:25133–25141.

Barrett, A. J., and P. M. Starkey. 1973. The interaction of α_2-macroglobulin with proteinases. *Biochem. J.* 133:709–712.

Binnig, G., C. F. Quate, and Ch. Gerber. 1986. Atomic force microscope. *Phys. Rev. Lett.* 56:930–933.

Brewer, J. W., T. D. Randall, R. E. P. Parkhouse, and R. B. Corley. 1994. IgM hexamers? *Immunol. Today.* 15:165–168.

Bustamante, C., D. Erie, and D. Keller. 1994. Biochemical and structural applications of scanning probe microscopy. *Curr. Opin. Struct. Biol.* 4:750–760.

Bustamante, C., D. Keller, and G. Yang. 1993. Scanning force microscopy of nucleic acids and nucleoprotein assemblies. *Curr. Opin. Struct. Biol.* 3:363–372.

Bustamante, C., J. Vesenka, C. L. Tang, W. Rees, M. Guthod, and D. Keller. 1992. Circular DNA molecules imaged in air by scanning force microscopy. *Biochemistry.* 31:22–26.

Carayannopoulos, L., and D. Capra. 1993. Immunoglobulins: structure and function. *In* Fundamental Immunology, 3rd Ed. W. E. Paul, editor. Raven, New York.

Delain, E., F. Pochon, M. Barry, and F. van Leuven. 1992. Ultrastructure of α_2-macroglobulins. *Electron Microsc. Rev.* 5:231–281.

Dodge, J. T., C. Mitchell, and D. J. Hanahan. 1962. The preparation and chemical characteristics of hemoglobin free ghosts of human erythrocytes. *Arch. Biochem.* 100:119–130.

Echlin, P. E. 1992. Low Temperature Microscopy and Analysis. Plenum, New York.

Edidin, M. 1993. Patches and fences: probing for plasma membrane domains. *J. Cell Sci. Suppl.* 17:165–169.

Elmer, T. 1980. Glass surfaces. *In* Silylated Surfaces. D. E. Leiedemn and W. T. Collins, editors. Gordon and Breach, New York. 11–12.

Engel, A. 1991. Biological applications of scanning probe microscopes. *Annu. Rev. Biophys. Chem.* 20:79–108.

Flicker, P. F., T. Walliman, and P. Vibert. 1983. Electron microscopy of scallop myosin. *J. Mol. Biol.* 169:723–741.

Hallett, P., G. Offer, and M. J. Miles. 1995. Atomic force microscopy of the myosin molecule. *Biophys. J.* 68:1604–1606.

Han, W., J. Mou, J. Sheng, J. Yang, and Z. Shao. 1995. Cryo atomic force microscopy: a new approach for biological imaging at high resolution. *Biochemistry.* 34:8215–8220.

Hansma, H. G., and J. Hoh. 1994. Biomolecular imaging with the atomic force microscope. *Annu. Rev. Biophys. Biomol. Struct.* 23:115–128.

Hansma, P. K., J. P. Cleveland, M. Radmancher, D. A. Walters, P. E. Hillner, M. Bezanilla, M. Fritz, D. Vie, H. G. Hansma, C. B. Prater, J. Massie, L. Fukunaka, J. Gurley, and V. Elings. 1994. Tapping mode atomic force microscopy in liquids. *Appl. Phys. Lett.* 64:1738–1740.

Hansma, H. G., D. E. Laney, M. Bezanilla, R. L. Sinsheimer, and P. K. Hansma. 1995. Applications for atomic force microscopy of DNA. *Biophys. J.* 68:1672–1677.

Henderson, E., P. G. Hayelon, and D. S. Sakaguchi. 1992. Actin filament dynamics in living glial cells imaged by atomic force microscopy. *Science.* 257:1944–1946.

Henderson, R. 1995. The potential and limitations of neutrons, electrons and X-rays for atomic resolution microscopy of unstained biological molecules. *Q. Rev. Biophys.* 28:171–194.

Hoh, J., and C. Schoenenberger. 1994. Surface morphology and mechanical properties of MDCK monolayers by atomic force microscopy. *J. Cell Sci.* 107:1105–1114.

Ikai, A., M. Kikuchi, and M. Nishigai. 1990. Internal structure of ovomacroglobulin studied by electron microscopy. *J. Biol. Chem.* 265: 8280–8284.

Ill, C. R., V. M. Keivens, J. E. Hale, K. K. Nakamura, R. A. Jue, S. Cheng, E. D. Melcher, B. Drake, and M. C. Smith. 1993. A COOH-terminated peptide confers regiospecific orientation and facilitates atomic force microscopy of an IgG1. *Biophys. J.* 64:919–924.

Keller, D., and C. Chi-Chung. 1992. Imaging steep, high structures by scanning force microscopy with electron beam deposited tips. *Surface Sci.* 268:333–339.

Larquet, E., N. Boisset, F. Pochon, and J. Lamy. 1994. Architecture of native human α_2-macroglobulin studied by cryoelectron microscopy and three dimensional reconstruction. *J. Struct. Biol.* 113:87–98.

Lindsay, S. M.. 1993. Biological applications of scanning probe microscopy. *In* Scanning Tunneling Microscopy and Spectroscopy: Theory, Techniques and Applications. D. A. Bonnell, editor. VCH, New York.

Marshall, L. B., N. L. Figler, and S. L. Gonias. 1992. Identification of α_2-macroglobulin conformational intermediates by electron microscopy and image analysis. *J. Biol. Chem.* 267:6347–6352.

Metzger, H. 1992. Transmembrane signaling: the joy of aggregation. *J. Immunol.* 149:1477–1487.

Muller, D. J., F. A. Schabert, G. Buldt, and A. Engel. 1995. Imaging purple membranes in aqueous-solution at subnanometer resolution by atomic force microscopy. *Biophys. J.* 68:1681–1686.

Mou, J., J. Yang, and Z. Shao. 1993. An optical detection low temperature atomic force microscope at ambient pressure for biological research. *Rev. Sci. Instrum.* 64:1483–1488.

Mou, J., D. M. Czajkowsky, Y. Zhang, and Z. Shao. 1995a. High resolution atomic force microscopy of DNA: the pitch of the double helix. *FEBS Lett.* 371:279–282.

Mou, J., J. Yang, and Z. Shao. 1995b. Atomic force microscopy of cholera toxin B oligomer bound to biologically relevant lipids. *J. Mol. Biol.* 248:507–512.

Parkhouse, R. M., B. A. Askonas, and R. R. Dourmashkin. 1970. Electron microscopic studies of mouse immunoglobulin M structure and reconstitution following reduction. *Immunology.* 18:575–584.

Perkins, S. J., A. S. Nealis, B. J. Sutton, and A. Feinstein. 1991. Solution structure of human and mouse immunoglobulin M by synchrotron X-ray scattering and molecular graphics modeling. *J. Mol. Biol.* 221: 1345–1366.

Polak, J., and I. Varndell. 1984. Immunolabeling for Electron Microscopy. Elsevier, Amsterdam.

Poljak, R. J. 1975. X-ray diffraction studies of immunoglobulins. *Adv. Immunol.* 21:1–33.

Prater, C. B., M. R. Wilson, J. Garnaes, J. Masie, V. B. Elings, and P. K. Hansma. 1991. Atomic force microscopy of biological samples at low temperature *J. Vac. Sci. Technol.* B9:989–991.

Putman, C. A., K. O. van der Wert, B. G. de Grooth, N. F. Hulst, and J. Creve. 1994. Viscoelasticity of living cells allows high resolution imaging by tapping mode atomic force microscopy. *Biophys. J.* 67: 1749–1753.

Roberts, C. J., P. M. Williams, J. Davies, A. C. Dawkes, J. Sefton, J. C. Edwards, A. G. Haymes, C. Bestwick, M. C. Davies, and S. J. B. Tendler. 1995. Real space differentiation of IgG and IgM antibodies deposited on microtiter wells by scanning force microscopy. *Langmuir.* 11:1822–1826.

Rogers, W., and M. Glaser. 1993. Distributions of proteins and lipids in erythrocyte membrane. *Biochemistry.* 32:12591–12598.

Sambrook, J., E. F. Fritsch, and T. Maniatis. 1989. Molecular Cloning: A Laboratory Manual, 2nd Ed. Cold Spring Harbor Laboratory, Cold Spring Harbor, New York.

Schabert, F. A., C. Henn, and A. Engel. 1995. Native *E. coli* Ompf porin surfaces probed by atomic force microscopy. *Science.* 268:92–94.

Shao, Z., J. Mou, D. M. Czajkowsky, J. Yang, and J. Y. Yuan. 1996. Biological atomic force microscopy: what is achieved and what is needed. *Adv. Phys.* 45:1–86.

Shao, Z., and A. P. Somlyo. 1995. Stereo representation of atomic force micrographs: optimizing the view. *J. Microsc.* 180:186–188.

Shao, Z., and J. Yang. 1995. Progress in high resolution atomic force microscopy in biology. *Q. Rev. Biophys.* 28:195–251.

Shao, Z., J. Yang, and A. P. Somlyo. 1995. Biological atomic force microscopy: from microns to nanometers and beyond. *Annu. Rev. Cell Dev. Biol.* 11:241–265.

Sheets, E. D., R. Simson, and K. Jacobson. 1995. New insights into membrane dynamics from the analysis of cell surface interactions by physical methods. *Curr. Opin. Cell Biol.* 7:707–714.

Shuttack, M. B., M. G. L. Gustafsson, K. A. Fisher, K. C. Yanagimoto, A. Veis, R. S. Bhatnagar, and J. Clarke. 1994. Monomeric collagen imaged by cryogenic force microscopy. *J. Microsc.* 174:RP1–2.

Smythe, E., and G. Warren. 1991. The mechanism of receptor-mediated endocytosis. *Eur. J. Biochem.* 202:689–699.

Thimonier, J., J. P. Chauvin, J. Barbet, and J. Roccaserra. 1995. Preliminary studies of an immunoglobulin M by near field microscopies. *J. Trace Microprobe Tech.* 13:353–359.

Thomson, N. H., M. Fritz, M. Radmacher, J. P. Cleaveland, C. F. Schmidt, and P. K. Hansma. 1996. Protein tracking and detection of protein motion using atomic force microscopy. *Biophys. J.* 70:2421–2431.

Urry, D. W.. 1988. Entropic elastic processes in protein mechanisms. I. Elastic structure due to an inverse temperature transition and elasticity due to internal chain dynamics. *J. Protein Chem.* 7:1–34.

Vaerman, J. P., A. Langendries, and C. van der Maelen. 1995. Homogenous IgA monomers, dimers, trimers and tetramers from the same IgA myeloma serum. *Immunol. Invest.* 24:631–641.

Wang, J. F., and T. R. Cech. 1992. Tertiary structure around the guanosine binding site of the Tetrahymena ribozyme. *Science.* 256:526–529.

Wong, T. M. H., and P. Descouts. 1995. Atomic force mciroscopy under liquid: a comparative study of three different AC mode operations. *J. Microsc.* 178:7–13.

Yang, J., J. Mou, and Z. Shao. 1994a. Structure and stability of pertussis toxin studied by in situ atomic force microscopy. *FEBS Lett.* 338:89–92.

Yang, J., J. Mou, and Z. Shao. 1994b. Molecular resolution atomic force microscopy of soluble proteins. *Biochim. Biophys. Acta.* 1199:105–114.

Yang, J., K. Takeyasu, and Z. Shao. 1992. Atomic force microscopy of DNA molecules. *FEBS Lett.* 301:173–176.

Yang, J., L. K. Tamm, A. P. Somlyo, and Z. Shao. 1993a. Promises and problems of biological atomic force microscopy. *J. Microsc.* 171: 183–198.

Yang, J., L. K. Tamm, T. W. Tillack, and Z. Shao. 1993b. New approach for atomic force microscopy of membrane proteins: the imaging of cholera toxin. *J. Mol. Biol.* 229:286–290.